UNCLASSIFIED

NACA

RESEARCH MEMORANDUM

for the

Air Materiel Command, U. S. Air Force

WIND-TUNNEL INVESTIGATION OF THE LOW-SPEED STATIC

STABILITY AND CONTROL CHARACTERISTICS OF

A MODEL OF BELL MX-776

By

M. J. Queijo and W. H. Michael, Jr.

Langley Aeronautical Laboratory
Langley Air Force Base, Va.

NATIONAL ADVISORY COMMITTEE
FOR AERONAUTICS
WASHINGTON
JUL 6 1949

3 1176 01437 9987

NATIONAL ADVISORY COMMITTEE FOR AERONAUTICS

RESEARCH MEMORANDUM

for the

Air Materiel Command, U. S. Air Force

WIND-TUNNEL INVESTIGATION OF THE LOW-SPEED STATIC

STABILITY AND CONTROL CHARACTERISTICS OF

A MODEL OF BELL MX-776

By M. J. Queijo and W. H. Michael, Jr.

SUMMARY

An investigation has been made in the Langley stability tunnel to determine the low-speed static stability and control characteristics of a model of the Bell MX-776. The results of the investigation indicated that the basic model configuration was longitudinally stable in the angle-of-attack range from about -16° to 16° but that the stability was a minimum near 0° angle of attack. The data indicated an aerodynamic-center position about 0.64 body diameters behind the center of gravity at low angles of attack. Reduction in the size of the front horizontal fins increased the longitudinal stability. With 20 percent of the span of the normal front horizontal fins cut off, the aerodynamic center was about 1.04 body diameters behind the center of gravity, and with front horizontal fins having the same area as the front vertical fins, the aerodynamic center was 2.26 body diameters behind the center of gravity (at low angles of attack).

With a simulated elevator deflection of 30°, the basic model configuration trimmed at about 11° angle of attack, and at this trim point, the model was more stable, longitudinally (aerodynamic center 1.33 body diameters behind the center of gravity), than at the trim point with elevators undeflected. With elevators undeflected, the model was directionally stable in the range of angles of attack from -11° to 11°; however, with a simulated elevator deflection of 30° the model became directionally unstable at about 9° angle of attack, which is lower than the angle of attack required for longitudinal trim.

INTRODUCTION

At the request of the Air Materiel Command, U. S. Air Force, the Langley stability-tunnel section has conducted a wind-tunnel investigation of the low-speed static stability and control characteristics of a $\frac{1}{3.7}$-scale model of the Bell MX-776. Preliminary flight tests (reference 1) of an earlier configuration had indicated longitudinal instability at low angles of attack at both subsonic and supersonic speeds. Unpublished data from low-speed tunnel tests (made in the Langley stability tunnel) of this earlier configuration also showed longitudinal instability at low angles of attack.

After results from reference 1 were known, the Bell MX-776 model was modified to provide better longitudinal characteristics. Before conducting flight tests of the model of the modified version, it was thought advisable to investigate both the longitudinal and lateral stability characteristics by means of low-speed wind-tunnel tests. On the basis of previous experience it was believed that these tests would provide information directly applicable to flight at subsonic speeds and should provide at least a qualitative indication of the behavior of the model at supersonic speeds.

The model used in this investigation was provided the NACA by the MX-776 contractor for tests at the pilotless aircraft testing station, Wallops Island, Va. The present paper gives results of an investigation which had as its primary purpose the determination of longitudinal and lateral stability characteristics of the model. A limited amount of information on longitudinal and lateral control characteristics also has been obtained.

SYMBOLS AND COEFFICIENTS

All forces and moments are given with respect to the system of wind axes shown in figure 1. The origin of the axes is the center of gravity of the model. The symbols and coefficients used herein are defined as follows:

C_L lift coefficient (L/qS_F)

C_D drag coefficient (D/qS_F)

C_Y side-force coefficient (Y/qS_F)

$$C_{Y_\psi} = \frac{\partial C_Y}{\partial \psi}$$

$$C_{l_\psi} = \frac{\partial C_l}{\partial \psi}$$

$$C_{n_\psi} = \frac{\partial C_n}{\partial \psi}$$

APPARATUS

The tests of this investigation were made in the 6- by 6-foot curved-flow test section of the Langley stability tunnel. The model used was of approximately $\frac{1}{3.7}$-scale and was one of the models provided to NACA for flight tests at the pilotless aircraft testing station, Wallops Island, Va. The basic (normal) model configuration of the present investigation is shown in figure 2. The body of the model was constructed primarily of balsa wood and contained metal castings into which metal fins were securely bolted. A steel tube was inserted in the body of the model and was clamped tightly in position. The tube was then bolted to a single strut support which was in turn fastened to a six-component balance system. A drawing of the model in the Langley stability tunnel is given as figure 3.

Three sizes of front horizontal fins were used in this investigation: the normal fins, the normal fins with 20 percent of the exposed span cut off at the tips, and small fins which were the same size as the front vertical fins. The dimensions of the various front horizontal fins are given in figure 4.

None of the fins supplied with the model had moveable control surfaces; hence, in order to obtain some indication of the elevator and aileron effectiveness, wedges were made which could be attached to the surfaces to simulate full-span control deflections (fig. 5). The wedge chords were 25 percent of the wing chords. The elevators of this model were on the front horizontal fins, and the ailerons were on the rear vertical fins.

In addition to the wedges, a new set of rear vertical fins were built. These fins were made up of a $\frac{1}{16}$-inch-thick sheet of duralumin

sandwiched between two sections of balsa wood so that the over-all fin dimensions were the same as those of the original vertical fins. The duralumin sheet was perforated along the three-quarter-chord line so that it could be bent there to simulate deflections of a full-span quarter-chord plain flap. The perforations were plugged during the tests. The details of the built-up fins are shown in figure 5.

TESTS

Two series of tests were made, one to determine the static longitudinal stability and control characteristics of the model and the other to determine the static lateral stability and control characteristics. In order to obtain a complete evaluation of the forward and rear fins, tests were made of the complete model, the model with forward fins removed, and the model with the rear fins removed. The characteristics of the body alone also were obtained.

Angle-of-yaw tests were made by pitching the model after it had been rotated 90° about its longitudinal axis.

All tests but the aileron tests were made with and without the dummy strut and fairing. The aileron tests were made with the model mounted on its side and with the rear horizontal fins removed in order to eliminate support-strut interference effects as completely as possible. Various angles of attack were obtained by yawing the model in the tunnel. Because of the instability of the model with the rear horizontal fins removed, severe oscillations started at angles of attack of about 7°; hence results are presented only for angles of attack up to 6°.

All tests were made at a dynamic pressure of 64.3 pounds per square foot, which corresponds to a Reynolds number of about 700,000 (sea-level conditions) based on the maximum body diameter (0.473 ft).

CORRECTIONS

Corrections were applied to all the data (except aileron test data) to account for support-strut interference. No corrections were applied to the aileron data because the ailerons were always well above the support strut and hence corrections were believed unnecessary. The pitching-moment and yawing-moment coefficients were corrected for

jet-boundary effects (determined by use of reference 2) and these corrections (given in the following table) were added to the calculated coefficients.

Horizontal fins		Vertical fins		$\Delta C_m = k_1\alpha$	$\Delta C_n = k_2\psi$
Front	Rear	Front	Rear	k_1	k_2
Normal	Normal	Normal	Normal	0.0453	0.00853
20-percent cut	Normal	Normal	Normal	.0435	.00853
Small	Normal	Normal	Normal	.0358	.00853
None	Normal	Normal	Normal	.0284	.00853
Normal	None	Normal	Normal	-.00509	.00853
20-percent cut	None	Normal	Normal	-.00363	.00853
Small	None	Normal	Normal	-.000664	.00853
Normal	Normal	None	Normal	.0453	.00573
Normal	Normal	Normal	None	.0453	-.000673
None	None	None	None	0	0

The angles of attack and of yaw were corrected for flexibility of the model support strut.

RESULTS AND DISCUSSION

Presentation of Results

All data are presented about the wind axes (fig. 1). The longitudinal stability characteristics of several model configurations are shown in figures 6 to 8. The variations of downwash angle with angle of attack near the rear horizontal fins, caused by the front horizontal fins, are shown in figure 9. The effects of simulated elevator deflection on the longitudinal characteristics are shown in figures 10 and 11. Increments of section lift coefficient resulting from various deflections of plain and split trailing-edge flaps (data from reference 3) are shown in figure 12. These data are used to evaluate the results obtained by simulating control deflections by means of wedges.

Lateral stability characteristics for various configurations are shown in figure 13; and figure 14 shows the variation of sidewash angle with angle of yaw in the vicinity of the rear vertical fins of the complete model. The lateral stability characteristics for the basic configuration at various angles of attack and angles of yaw are given in figures 15 and 16 for zero elevator deflection. The aerodynamic

characteristics of the basic configuration with simulated elevator deflection are presented in figure 17. In figure 18 are shown the lateral stability derivatives C_{Y_ψ}, C_{l_ψ}, and C_{n_ψ} (obtained from the data of figures 16 and 17) for the basic configuration with elevators neutral and deflected 30°. Increments of rolling moment produced by aileron deflections are shown in figure 19.

Longitudinal Characteristics

Stability.— The longitudinal stability characteristics of several configurations are shown in figure 6. The data show that the complete model with normal fins is longitudinally stable in the angle—of—attack range from −16° to 16°. The pitching—moment curve (plotted against angle of attack) for the normal configuration is nonlinear, and the stability is lower near 0° angle of attack. Reduction in the area of the front horizontal fins increased the stability and tended to make the pitching—moment curves more linear.

The pitching—moment data for three complete configurations are replotted against lift coefficient in figure 7. These curves are somewhat more linear than the curves of C_m against α because the C_L—against—α data showed nonlinearities similar to the C_m—against—α data. The slopes of the pitching—moment curves of figure 7 (measured at $C_L = 0$) indicate aerodynamic—center positions of 0.64, 1.04, and 2.26 body diameters behind the center of gravity (mounting point) for the model with normal front horizontal fins, 20—percent cut fins, and small fins, respectively.

Data obtained for various model configurations with the rear horizontal fins removed are presented in figure 8. The data of the pitching—moment curves of figures 6 and 8 have been used to calculate the effective downwash angle in the vicinity of the rear horizontal fins (fig. 9). This is referred to as the effective downwash angle since no attempt has been made to account for any possible effects of the forward fins on the dynamic pressure at the rear horizontal fins. The results presented in figure 9 show that for the model with normal fins, the downwash angle ϵ varied rapidly with angle of attack for values of α near 0°. It appears, therefore, that the nonlinearities observed in the pitching—moment curves of figure 6 result largely from the variation of downwash angle with angle of attack.

Control.— The effects on C_L, C_D, and C_m of simulating an elevator deflection by adding 30° wedges to the forward horizontal fins are shown in figure 10. The increments in C_L and C_m caused by the

wedges are shown in figure 11. For positive angles of attack up to about 12° the wedges produced almost constant increments in pitching-moment coefficient and lift coefficient. In the negative angle-of-attack range, the pitching-moment increment shows a large decrease as the angle of attack is made more negative. It is believed that wedges provide a more valid indication of plain-flap deflections when the angle of attack and flap deflection are of the same sign.

Since the elevators of the full-scale missile are of the plain-flap type, it is necessary to determine the relative effectiveness of wedges and plain flaps. It is known that wedges generally exhibit the same aerodynamic characteristics as split flaps; hence if the relative effectiveness of plain flaps and split flaps is known, then the relative effectiveness of plain flaps and wedges can be found. A comparison of the effectiveness of plain flaps and split flaps, as determined from two-dimensional data, can be obtained from reference 2, and such a comparison is presented herein as figure 12. The figure compares plain and split-flap effectiveness for various flap deflections and angles of attack. For deflections of 30°, the two types of flaps have about the same effectiveness, and for smaller deflections the plain flaps are more effective than split flaps. For positive angles of attack, therefore, it might be expected that 30° wedges provide almost the same effectiveness as 30° deflection of plain flaps. With 30° simulated flap deflection, the model trims at about 11° angle of attack and has greater longitudinal stability at this trim point (aerodynamic-center position located 1.33 body diameters behind center of gravity) than at the trim point with 0° flap deflection.

Lateral Characteristics

Stability.- The lateral stability characteristics of several model configurations at zero angle of attack are shown in figure 13. The complete model (normal configuration) is directionally stable at zero angle of attack, in the yaw range from $\psi = -14°$ to $\psi = 14°$, but stability is a minimum at 0° angle of yaw. The data of figure 13 were used to compute the effective sidewash angles in the vicinity of the rear vertical fins, and the results are shown in figure 14. The figure shows the largest variation of sidewash angle with angle of yaw in the yaw range from -4° to 4°. For larger positive yaw angles the sidewash angle is very nearly constant. It appears, therefore, that the nonlinearity of the curve of C_n against ψ for the basic configuration results largely from the sidewash angle.

The lateral stability characteristics of the normal configuration at various angles of attack are shown in figure 15. The model appears to be almost neutrally stable at angles of attack of about ±9.2°. The

unsymmetric appearance of the rolling-moment curves of figure 15 probably is caused by inability to eliminate completely the effects of the support strut.

Data obtained by pitching the model through an angle-of-attack range for angles of yaw of 0°, and $\pm 5^\circ$ for elevator deflections of 0° and 30° are shown in figures 16 and 17, respectively. The lateral-stability derivatives C_{n_ψ}, C_{l_ψ}, and C_{Y_ψ} obtained from these data are presented in figure 18. With elevators neutral, these results (fig. 18) confirm a point previously noted — that the directional stability becomes neutral near $\alpha = \pm 10^\circ$. Beyond these limits the model is directionally unstable. Deflection of the elevators tended to reduce the directional stability at positive angles of attack, and thus neutral stability was obtained at about 9°. This result is in agreement with results of tests (unpublished) from the Langley free-flight tunnel, which showed that an increase in incidence of the forward horizontal tail of a canard-type model tended to reduce the stabilizing effect of a vertical tail located at the rear of a model. The data for this model indicated directional instability in the trimmed condition with 30° elevator deflection.

Control.— The lateral controls (ailerons) were investigated briefly. Deflections of ailerons on the built-up rear vertical fins resulted in the increments of rolling-moment coefficient shown in figure 19(a). Variations in angle of attack up to 6° appear to be of little importance. Comparison of the increment of rolling-moment coefficient obtained by 15° deflection of the ailerons on built-up fins and the increments obtained with 15° wedges are shown in figure 19(b). Wedges produced about the same effect on either the normal or the built-up fins, but in either case, the wedges were only about two-thirds as effective as the plain-flap type of aileron. The comparison of effectiveness of plain and split flaps given in figure 12 (for $\alpha = 0^\circ$) indicates that the increment in rolling moment obtained by wedges should be lower than that from plain flaps; however, test results with wedges were even lower than expected.

It should be remembered that the aileron tests were made with the rear horizontal fins removed in order to eliminate the effects of support interference as completely as possible. The effectiveness of the ailerons in the presence of the rear horizontal fins would be expected to be slightly lower than that obtained (because of the interference of the rear horizontal fins).

CONCLUSIONS

The results of tests made to determine the low-speed stability and control characteristics of a model of the Bell MX-776 have led to the following conclusions:

1. The basic model configuration is longitudinally stable in the angle-of-attack range from about -16° to 16°, but the stability was a minimum near 0° angle of attack. The data indicate an aerodynamic-center position about 0.64 body diameters behind the center of gravity at low angles of attack.

2. Reduction in the size of the front horizontal fins increased the longitudinal stability. The normal front horizontal fins with 20 percent of the exposed span cut off and the small front horizontal fins showed aerodynamic-center positions of 1.04 and 2.26 body diameters behind the center of gravity, respectively.

3. With a simulated elevator deflection of 30°, the airplane trimmed at about 11° angle of attack, and at this trim point the model was more stable, longitudinally (aerodynamic-center position located 1.33 body diameters behind center of gravity) than at the trim point with elevators undeflected.

4. The model was directionally stable, with elevators neutral, in the angle-of-attack range from -11° to 11° and was unstable outside this range. With elevators deflected 30° the model became directionally unstable at about 9° angle of attack, which is lower than the angle of attack for longitudinal trim.

Langley Aeronautical Laboratory
    National Advisory Committee for Aeronautics
        Langley Air Force Base, Va.

M. J. Queijo
Aeronautical Research Scientist

W. H. Michael, Jr.
Aeronautical Engineer

Approved:
        Thomas A. Harris
    Chief of Stability Research Division

jsf

REFERENCES

1. Michal, David H., and Mitcham, Grady L.: Preliminary Results of a
   Free-Flight Investigation of the Static Stability and Aileron
   Control Characteristics of $\frac{1}{6}$-Scale Models of the Bell MX-776.
   NACA RM SL9D21, U. S. Air Force, 1949.

2. Silverstein, Abe, and White, James A.: Wind-Tunnel Interference with
   Particular Reference to Off-Center Positions of the Wing and to
   the Downwash at the Tail. NACA Rep. 547, 1935.

3. Wenzinger, Carl J., and Harris, Thomas A.: Wind-Tunnel Investigation
   of an N.A.C.A. 23012 Airfoil with Various Arrangements of Slotted
   Flaps. NACA Rep. 664, 1939.

Figure 1.- System of wind axes. Arrows indicate positive directions
of forces, moments, and angles.

Figure 2.- Basic model configuration of the Bell MX-776 used in this investigation. All airfoils are 5-percent-thick symmetric wedges. All dimensions are in inches.

Figure 3.- Drawing of the model of the Bell MX-776 in the Langley stability tunnel.

Figure 4.- Dimensions of the front horizontal fins used in the investigation. All dimensions are in inches.

A A

$\frac{3}{4}$-chord line

Rear vertical fin

A' A'

Perforated along $\frac{3}{4}$-chord line

Rear vertical fin (built up)

Section A-A
(Not to scale)

Balsa wood

Dural rib

Section A'-A'
(Not to scale)

$\frac{c}{4}$

Wood

15°

Wedge

Figure 5.- Details of wedge and built-up rear vertical fins used to obtain aileron deflections.

C_D

.28
.24
.20
.16
.12
.8
.4
0

Configurations				
Symbol	Horizontal fins		Vertical fins	
	Front	Rear	Front	Rear
○	Normal	Normal	Normal	Normal
□	20% out	Normal	Normal	Normal
◇	Small	Normal	Normal	Normal
△	None	Normal	Normal	Normal
▽	None	None	None	None

C_L

8
6
4
2
0
-2
-4
-6

Configurations				
Symbol	Horizontal fins		Vertical fins	
	Front	Rear	Front	Rear
○	Normal	Normal	Normal	Normal
□	20% out	Normal	Normal	Normal
◇	Small	Normal	Normal	Normal
△	None	Normal	Normal	Normal
▽	None	None	None	None

Front Horizontal fins

—— Normal

— — — 20% cut

— — Small

C_m

Lift coefficient C_L

Configuration				
Symbol	Horizontal fins		Vertical fins	
	Front	Rear	Front	Rear
○	Normal	Normal	Normal	Normal
□	Normal	None	Normal	Normal
◇	20% cut	None	Normal	Normal
△	Small	None	Normal	Normal
▽	None	None	None	None

Figure 9.- Variation of effective downwash angle near the rear horizontal fins with angle of attack for three sizes of front horizontal fins.

Figure 11.- Increments of lift and pitching-moment coefficients caused by simulated elevator deflection of 30°. Basic configuration. $\psi = 0°$.

(a) $\delta_f = 10°$

(b) $\delta_f = 20°$

(c) $\delta_f = 30°$

Δc_2

Configurations				
Symbol	Horizontal fins		Vertical fins	
	Front	Rear	Front	Rear
○	Normal	Normal	Normal	Normal
□	Normal	Normal	None	Normal
◇	Normal	Normal	Normal	None
△	None	None	None	None

	Configurations			
	Horizontal fins		Vertical fins	
Symbol	Front	Rear	Front	Rear
○	Normal	Normal	Normal	Normal
□	Normal	Normal	None	Normal
◇	Normal	Normal	Normal	None
△	None	None	None	None

Figure 14.- Variation of effective sidewash angle with angle of yaw.
Basic model configuration. $\alpha = 0^\circ$.

α
(deg)

○ 9.1
□ 4.7
◇ -0.1
△ -4.7
▽ -9.2

NACA RM SL9G08

NACA RM SL9G08

α
(deg)

○   0
□   2
◇   4
△   6

.8

ΔC_l .4

0

0   4   8   12   16

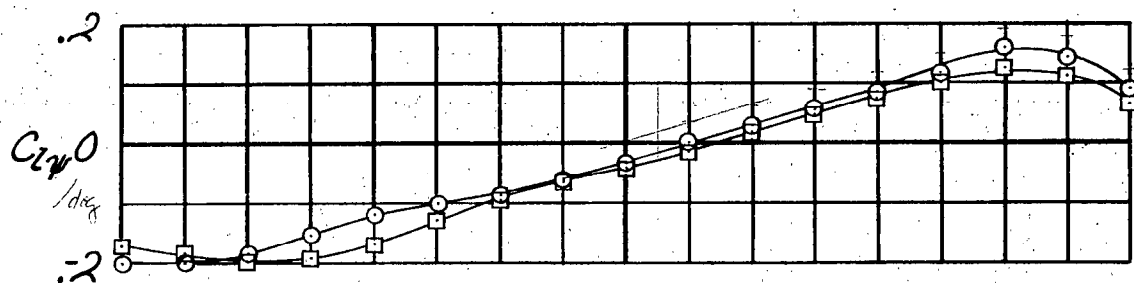Deflection of each aileron, δ_a, deg

(a) Increment of rolling-moment coefficient obtained by deflecting ailerons on built-up vertical fins.

○   Ailerons on built-up fins
□   Wedges on built-up fins
◇   Wedges on normal fins

.8

ΔC_l .4

0

0   2   4   6   8

Angle of attack, α, deg